NMR and Molecular Mechanics Study of Pyrethrins I and II

Joseph K. Rugutt,† Charles W. Henry III,† Scott G. Franzblau,‡ and Isiah M. Warner*,†

Department of Chemistry, Louisiana State University, Baton Rouge, Louisiana 70803, and Gillis W. Long Hansen's Disease Center, Baton Rouge, Louisiana 70894

Bioassay-directed fractionation of the organic extract of the Kenyan pyrethrum flowers (*Chrysanthemum cinerariaefolium* Vissiani) resulted in the isolation of two natural pyrethrin esters, pyrethrin **I** (P**I**) and pyrethrin **II** (P**II**) as the major constituents. These esters elicited inhibition of the multiple drug resistant (MDR) *Mycobacterium tuberculosis*. The high-field ^{1}H and ^{13}C nuclear magnetic resonance (NMR) chemical shifts of P**I** and P**II** were unequivocally assigned using modern two-dimensional (2D) proton-detected heteronuclear multiple-quantum coherence (HMQC) and heteronuclear multiple-bond correlation (HMBC) experiments. The conformations of both esters were deduced from $^{1}H-^{1}H$ vicinal coupling constants and confirmed by 2D nuclear Overhauser effect spectroscopy (NOESY). Computer molecular modeling (MM) studies revealed that P**I** and P**II** molecules adopt a "love-seat" conformation in chloroform ($CDCl_3$) solution.

Keywords: *Pyrethrum; Chrysanthemum cinerariaefolium; pyrethrins; vacuum−liquid chromatography; antimycobacteria; Mycobacterium tuberculosis; M. avium; nuclear magnetic resonance spectroscopy; molecular modeling; conformations*

INTRODUCTION

Tuberculosis (TB) is a serious healthcare menace and is the single most lethal infectious bacterial disease affecting mankind (Wayne, 1994). Historically, TB is a chronic, air-borne, contagious, debilitating disease that severely affects the respiratory tracts of humans. As a result of the emergence of the potentially incurable multiple drug resistant (MDR) strains of mycobacteria, the incidence of TB infection in the United States has steadily risen in the past decade (Houston and Fanning, 1994). Compounding the problem of the resurgence of TB is the association of TB with HIV infection among the highly vulnerable recreational drug users, children, street dwellers, the AIDS population, and immigrants from developing countries (Iseman, 1994). This medical crisis has rekindled interest in the search for antibiotics that inhibit or kill mycobacteria by novel mechanisms (Inderlied et al., 1993; Rastogi et al., 1981).

Nature is the prime source of many of the drugs currently in commercial use (Grange and Davey, 1990; Secoy et al., 1983). To unravel the scientific bases of the remedial effects of indigenous African plants that are used for the treatment of *Mycobacterium tuberculosis* infection, we recently began a program aimed at identifying new sources of chemotherapeutics. Initial bioassay-guided studies on the perennial pyrethrum flowers yielded several compounds that exhibited significant inhibition toward *M. tuberculosis* H37Rv and *M. avium* (Rugutt et al., 1999). The six major components of pyrethrum flowers (cinerin **I** (C**I**), jasmolin **I** (J**I**), pyrethrin **I** (P**I**), cinerin **II** (C**II**), jasmolin **II** (J**II**), and pyrethrin **II** (P**II**)) (Figure 1) are usually difficult to separate by column chromatography. Structurally, these

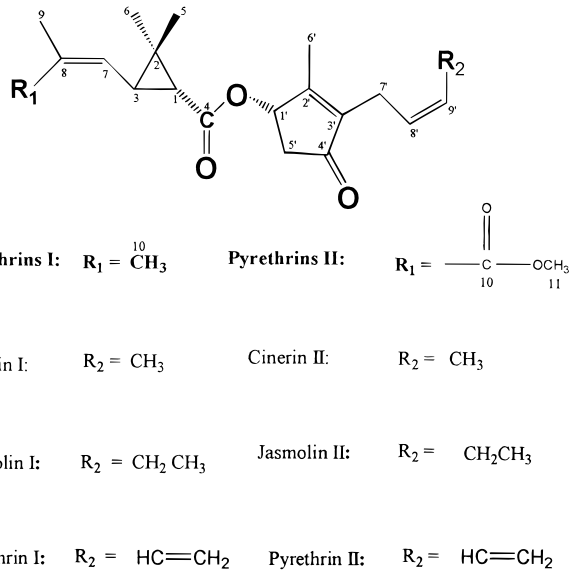

Figure 1. Structures of natural pyrethrins.

pyrethrin esters are respectively derived from a combination of three alcohols, cinerolone (**I**), jasmolone (**I**), and pyrethrolone (**I**), with two chrysanthemic acid (**II**) and pyrethric acid (**II**) (Patenden and Hemesley, 1973). It has been shown that the insecticidal activity (against household flies, human lice, mosquitoes, crop pests, and several ectoparasites) of pyrethrum extract is primarily due to the major components, P**I** and P**II** (McEldowney and Menary, 1988; Khambay et al., 1993; Johnston et al., 1989). Specifically, the chrysanthemates (P**I**, C**I**, J**I**) are lethal insecticides, whereas the pyrethrates (P**II**, C**II**, J**II**) cause rapid knockdown.

When pyrethrins are exposed to light and heat, they decompose (Chen and Casida, 1969). It has been shown that the photodecomposition products of P**I** and P**II** are the trans isomers resulting from the cis/trans isomerization of the double bond (C8′−C9′) in the butadiene

* To whom correspondence should be addressed. Phone: (225)-388-2829. Fax: (225)-388-3971. E-mail: Isiah.Warner@chemgate.chem.lsu.edu.

† Louisiana State University.

‡ Gillis W. Long Hansen's Disease Center.

10.1021/jf980660b CCC: $18.00
Published on Web 07/20/1999

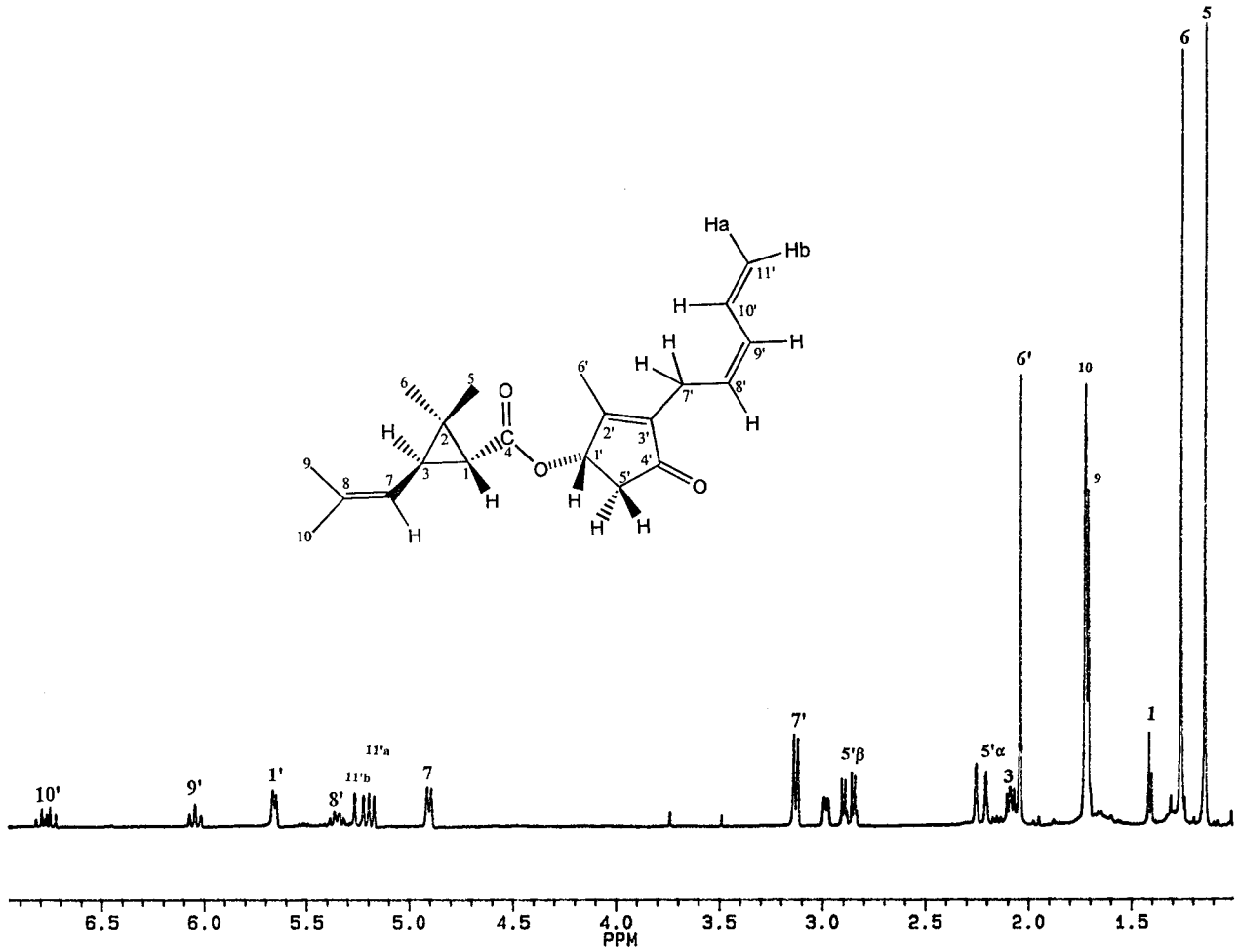

Figure 2. 400 MHz ^{1}H NMR spectrum of pyrethrin **I**.

side chain (Bullivant and Pattenden, 1976). The stabilities of pyrethrins to light under field and laboratory conditions can be improved by addition of UV stabilizers (Miskus and Andrews, 1972; Ueda et al., 1974; Sundaram and Curry, 1996). Since pyrethrin standards are not commercially available, the content and purity of the individual pyrethrins in pyrethrum flowers is usually determined by HPLC (Otieno et al., 1982; McEldowney and Menary, 1988), GC/MS (Pattenden et al., 1973), and NMR spectroscopy (Bramwell et al., 1969). The advantage of the NMR method is that only microgram quantities of the individual components are needed in order to prepare reference standards.

Pyrethrins are flexible molecules that continuously undergo fast conformational interconversion processes in solution. Their conformational properties are likely to be important in their mode of action against insects and bacteria (Ueda and Matsui, 1971; Elliot et al., 1974; Elliot, 1989). NMR is undoubtedly the most powerful technique for defining conformation of molecules in solution. For example, with the aim of understanding the mode of action of chiral fungicides (e.g., diclobutrazol, paclobutrazol, and triadimenol), their preferred conformations in solution have been deduced using the Karplus equation (Jackson and Sternhell, 1984). To date, the assignment of the resonances for cyclopropyl (Me-5 and Me-6) and vinyl *gem*-dimethyl groups of the natural pyrethrins has remained contradictory (Krishnamurthy and Casida, 1987; Bramwell et al., 1969; Crombie et al., 1975). In the present study, we used both molecular modeling (MM) and high-field NMR spectroscopic methods to definitely determine the conformations of P**I** and P**II** molecules in solution. The analytical process involved first the complete assignment of the ^{1}H NMR spectra for each molecule using 2D ^{1}H−^{1}H correlation spectroscopy (COSY). Second, we obtained all vicinal ^{1}H−^{1}H coupling constants ($^3J_{H-H}$) relevant to the conformational analysis. The conformation of each molecule was then derived by substitution of the $^3J_{H-H}$ values into the Karplus equation, which relates $^3J_{H-H}$ with the corresponding dihedral angles (Karplus, 1959; Karimi-Nejad et al., 1994). In addition, the concerted use of 2D NOESY (Bax and Davis, 1985), HMQC (Kessler et al., 1988), and HMBC (Bax and Summers, 1986) experiments provided unambiguous assignments of the cyclopropyl and vinyl *gem*-dimethyl groups of P**I** and P**II**.

MATERIALS AND METHODS

General. Pyrethrum flower concentrate (bulk no. 9819-4) was a gift sample from the Nakuru Pyrethrum Board of Kenya. Vacuum−liquid chromatographic (VLC) (Pelletier et al., 1986) separations of the concentrate were performed using silica gel (Rugutt et al., 1996). Ethyl acetate (EtOAc) and hexane were purchased from the Aldrich Chemical Co. (Milwaukee, WI) and distilled prior to use. Thin-layer chromatography (TLC) (Touchstone, 1995; Rugutt and Berner, 1998) was performed on precoated silica gel (Sil-G 25 UV_{254}) plates having a layer thickness of 0.25 mm. The TLC plates were developed using an EtOAc/hexane mixture (40:60 v/v) and made visible by spraying with a solution prepared by dissolving $CoCl_2 \cdot 6H_2O$ (2 g) in 10% aqueous H_2SO_4 (100 mL). Colored spots representing pyrethrin esters appeared on TLC plates after heating

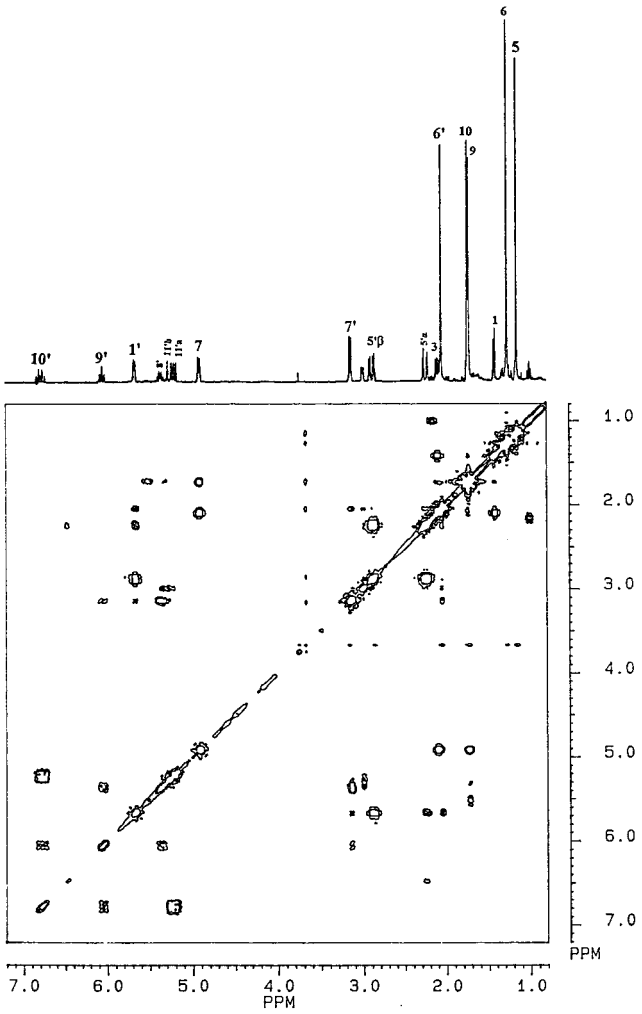

Figure 3. 2D $^1H-^1H$ COSY map of pyrethrin **I**.

at 100 °C for 1 min. Mass spectra were obtained on a Hewlett-Packard 5971A GC/MS spectrometer.

NMR Spectroscopy. One-dimensional (1D) ^1H and ^{13}C NMR spectra were recorded on an AMX Bruker spectrometer operating at 400 and 100 MHz Larmor frequencies, respectively (Diehl et al., 1972; Van Den and Van Waarde, 1996). The NMR spectra of pyrethrin esters (5 mg) contained in 5 mm outer diameter NMR tubes were recorded in the deuterium locked mode without spinning to reduce T_1 noise. Deuterated chloroform ($CDCl_3$; δ_H 7.24 ppm, δ_C 77.0 ppm) dispensed from sealed ampules was used as a solvent. The NMR data of P**II** (spectra not shown) were similar to those of P**I** (Figures 2−6 and Tables 1 and 2). Chemical shifts are expressed in δ (ppm) scale downfield from TMS (internal reference standard; δ_{TMS} 0 ppm). The coupling constants ($^3J_{H-H}$) are given in hertz (Hz). Proton chemical shifts are given with two decimal places in order to make certain distinctions for signal assignments especially concerning the H-9 and H-10 of P**I** and Hα-5′ and H-3 of P**II**. Typical ^1H NMR acquisition parameters were as follows: data set size, 16K; spectral width, 5400 Hz; 90° radio frequency pulse, 7.0 μs; recycling delay between transients, 2.0 s. Adequate signal-to-noise (S/N) ratios in the ^1H NMR spectra were achieved after 32 transients. Unless otherwise specified, temperature was always 298 K. Two-dimensional $^1H-^1H$ COSY and NOESY (Bax and Davis, 1985; Seebach et al., 1996) experiments were recorded on a Bruker AMX 400 MHz spectrometer. The following acquisition parameters were used. COSY: recycling delay (D1), 1.5 s; dummy scans (DS) = 4; number of scans (NS) = 64; D0 increment (D0) = 3 μs; spectral width in F2 = 2400 Hz, and in F1 = 1200 Hz; temperature = 298 K. The data set sizes were 512w in F1 and 1K in F2, and the data were zero-filled in F1 before subjecting to 2D Fourier transformation to yield a 1K × 1K data matrix. The resulting spectra were then processed using a sine-bell window function in F1 and F2 (WDW = s), and the data were diagonally symmetrized. NOESY: 512 × 512 data matrix size; time domain (td) = 512 in F1 and 1024 in F2; D1 = 2 s; D0 = 3 μs; NS = 96; mixing time (τ_m) = 800 ms. The ^1H-detected experiments, HMQC (Kessler et al., 1988), and HMBC (Bax and Summers, 1986) were recorded on a Bruker ARX 300 MHz spectrometer using the literature pulse sequences. The data were processed with Bruker XWIN-NMR software operating on a Silicon Graphics Indigo workstation (Silicon Graphics Inc., Bruker Co.). The acquisition parameters used were as follows. HMQC: 512 × 512 data matrix; td = 512 in F1 and 1024 in F2; D1 = 2 s; NS = 48; DS = 4. HMBC: data matrix size; td = 512w in F1 and 1024 in F2; D1 = 2 s; NS = 64; DS = 16; D0 = 3 μs; the $^3J_{CH}$ low pass filter was set to 3.48 ms, and the delay for the evolution of long-range coupling (7.7 Hz) was set to 60 ms. The proton−carbon assignments were confirmed by ^{13}C DEPT experiments (Doddrell et al., 1982) and $^1H-^{13}C$ HMQC. In DEPT experiments, the spin−echo technique was used to edit the ^{13}C spectra, i.e., to separate ^{13}C spectra into methyl (CH_3), methylene (CH_2), methine (CH), and quaternary (C) carbons with varied proton polarization pulse angles (PΦ). In the DEPT 45 experiment, PΦ = 5.0 μs was used to obtain optimal intensities for the protonated carbons (Tables 1 and 2). The DEPT 90 experiment with PΦ = 10.0 μs identified the CH protons, while the DEPT 135 experiment with PΦ = 15.0 μs gave positive signals for the CH_2 and CH_3 groups and negative signals for the CH groups.

Computer Molecular Modeling (MM). In the present study, the NMR NOESY spectra of P**I** and P**II** showed through-space intramolecular interactions between several hydrogens that warranted molecular modeling investigation. Conformational analysis (Burkert and Allinger, 1982) was performed on a Silicon Graphics Iris 4D/20 workstation using SYBYL 6.3 (1991) molecular modeling software. Attempts to secure crystals of either P**I** or P**II** suitable for X-ray analysis failed. This was further supported by a search of the Cambridge Crystallographic Database (CCD) which did not yield crystal structures. Pyrethrin esters have three stereogenic centers (C-1, C-3, and C-1′) and may exist as mixtures of eight isomers (RRR, RRS, RSR, SRR, SSS, SSR, SRS, and RSS). In addition to these stereogenic sites, there is a cis/trans double bond site (C8′−C9′). The structure of P**I** whose stereochemistry (Figure 1, trans C3−C7; C1−R; C1′S) has been partially determined (Bramwell et al., 1969) was used as a starting point for energy minimizations. Using the "build/edit" function of SYBYL 6.3 program, the natural isomers (C3−R, C1−R, C-1′S, 8′Z) of P**I** and P**II** were constructed and energy minimized using Gasteiger−Hückel charge assignments and 10^4 iterations. The minimized structures were further subjected to approximately 25 dynamic annealing runs using various temperature regimes and Gasteiger−Hückel charge assignments. When the conformational energy converged (no lower energy determined), the lowest energy conformers were analyzed. The hydrogen−hydrogen distances of interest were calculated using the "measure" function of SYBYL program. When the distance was between a hydrogen and a methyl group, an average of the distances between the lone hydrogen and each of the methyl group hydrogens was determined and reported (Table 3).

Antimycobacterial Activity. The standard radiorespirometric bioassays were performed in the BACTEC 460 as described by Collins and Franzblau (1997). Briefly, stock solutions (10.24 mg/mL) of test compounds were prepared in DMSO, filter sterilized. Solutions of lower concentrations were obtained by serial dilution using DMSO as the solvent. Aliquots (50 μL) of each solution were added to a 4 mL of fresh BACTEC 12B broth (Becon Dickinson, Towson, MD) containing mycobacteria (*M. avium* and the drug-sensitive *M. tuberculosis* H37Rv). Drug and bacterial controls (diluted 1:100) were also included. Cultures containing the test compounds were incubated at 37 °C, and the growth indices were determined daily starting on the second day of incubation. The bioassays were completed within 10 days for both mycobac-

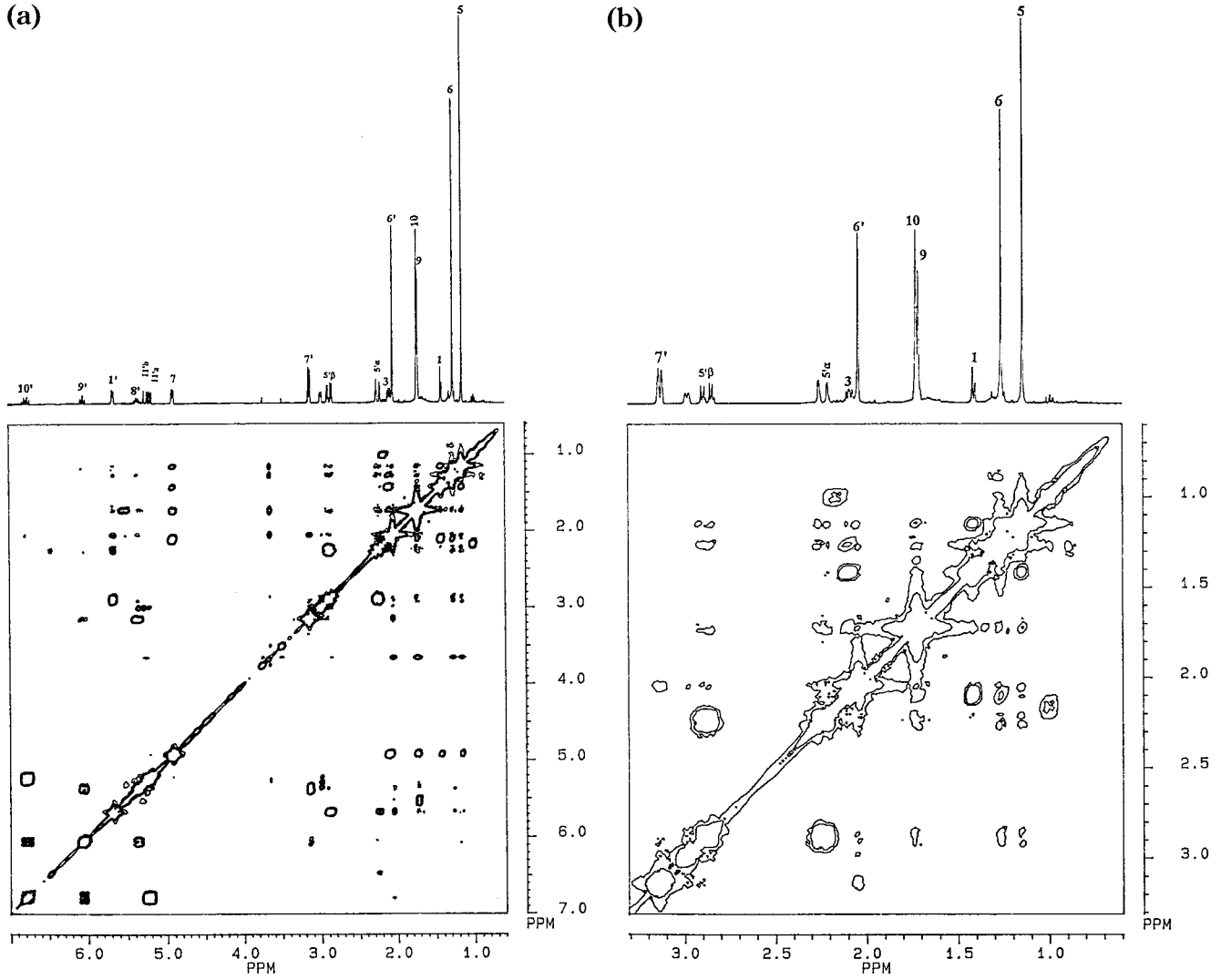

Figure 4. (a) 2D $^1H-^1H$ NOESY map of pyrethrin **I**. (b) Upfield region of NOESY map of pyrethrin **I**.

teria. The antimycobacterial activities for extracts and pure pyrethrins are expressed as percentage inhibition and minimum inhibitory concentrations (MICs), respectively. MIC is defined as the lowest concentration that inhibits the growth of 99% of the bacteria (Heifets, 1991).

RESULTS AND DISCUSSION

One-Dimensional (1D) NMR Studies. Encouraged by the antimycobacterial activity of pyrethrin esters (**PI** and **PII**), we further investigated their NMR behavior. Their high-field 1D ^1H and ^{13}C NMR data (Tables 1 and 2) are in agreement with the structures (Figure 1). However, dramatic and diagnostic differences occurred in the upfield regions of their ^1H NMR spectra. The three-bond coupling constants ($^3J_{H-H}$) were obtained from the ^1H NMR spectra. The vinyl coupling constants were similar to those reported in the literature (Bramwell et al., 1969), with marginal variations of about 0.01 ppm. Because the 1D spectra were complicated by the occurrence of resonances due to traces of other pyrethrins, several 2D NMR experiments were performed.

Two-Dimensional (2D) NMR Studies. For the first time, a combination of HMBC (Figure 6) and NOESY (Figure 4) experiments provided unambiguous assignments of the resonances for cyclopropyl and vinyl *gem*-dimethyl groups of P**I** and P**II**. The HMBC ("inverse COLOC") provided long-range $^1H-^{13}C$ coupling ($^nJ_{C-H}$; $n = 2-4$). Figure 6 shows the processed 2D HMBC spectrum for P**I**. The signals of quaternary carbon atoms were easily assigned (Tables 1 and 2) since the HMBC spectrum exhibited cross-peaks, which correlated nonprotonated carbon atoms to protons (two, three, and four bonds away). Two-dimensional NOESY experiments allowed simultaneous through-space connectivity of all protons to be established. In a typical 2D NOESY spectrum (Figure 4), the cross-peaks represent NOE and indicate that the protons, correlated by diagonal peaks, exhibit close spatial proximity (usually less than 5.0 Å) with each other. The standard ^1H NMR spectrum appears on the diagonal, while the NOE enhancements appear as off-diagonal peaks. The magnitude of the observed NOE is not only inversely proportional to the sixth power of the interproton distance in space (eq 1) but also depends on the effective rotational correlation times τ_c (Fesik, 1989):

$$\mathrm{NOE} \propto \{1/\langle r^6 \rangle\} f(\tau_c) \qquad (1)$$

Both P**I** and P**II** molecules are of intermediate size and undergo relatively rapid tumbling with a correlation time, τ_c, of approximately 10^{-10} s (Kessler et al., 1986). Therefore, to overcome the slow rate of NOE buildup and the low intensity of cross-peaks in the NOESY spectrum, a long mixing time of 800 ms was used. It is

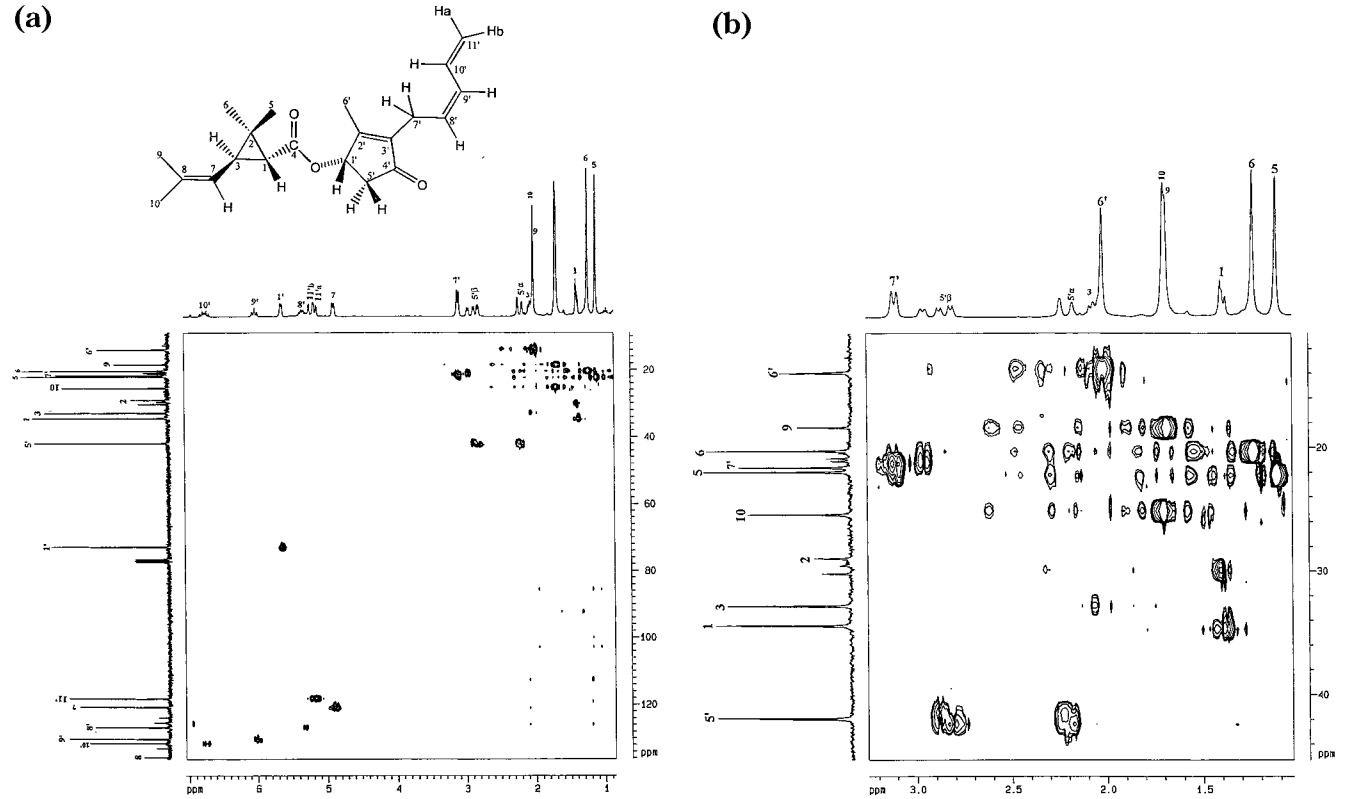

Figure 5. (a) 2D $^{1}H-^{13}C$ HMQC map of pyrethrin **I**. (b) Upfield region of HMQC map of pyrethrin **I**.

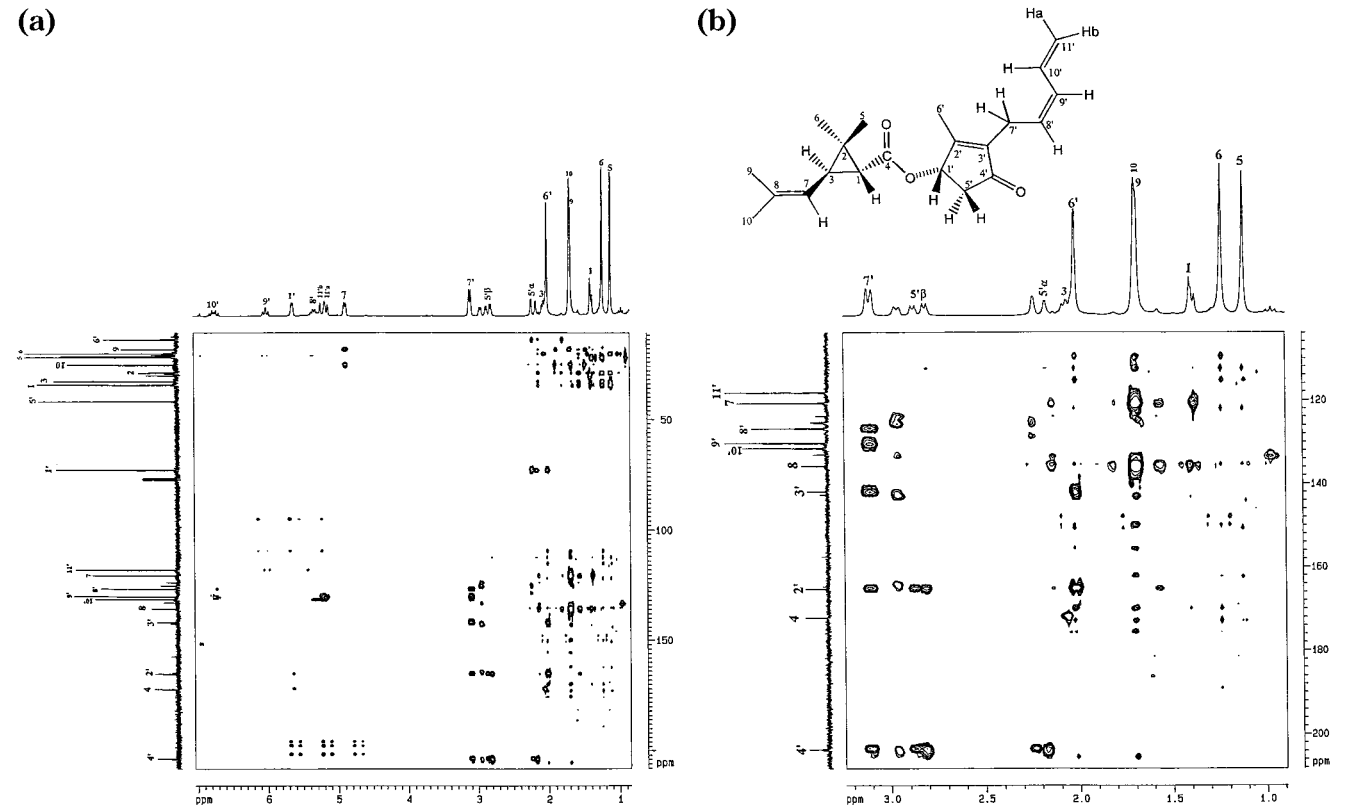

Figure 6. (a) 2D $^{1}H-^{13}C$ HMBC map of pyrethrin **I**. (b) Upfield region of HMBC map of pyrethrin **I**.

pertinent to mention here that the continued observation of cross-peaks in all NOESY spectra at different mixing times (between 400 and 800 ms) indicated that they were not due to artifacts. Phase cycling and small random fluctuation (5%) of mixing time were employed in order to effectively suppress COSY *J*-coupling cross-peaks due to zero-quantum (ZQ) and double-quantum (DQ) coherence transfers (e.g., in P**I**, the H9′, −H8′ cross-peak at {f1;f2} = {6.04, 5.36} ppm is significantly reduced). Despite the respectable time consumption of 2D NOESY experiments, several useful NOE cross-peaks were detected (Figure 7). The NOE cross-peak

Table 1. Summary of the Major Results of ^{1}H, ^{13}C, and HMBC Correlations of Pyrethrin I

position	δ^{13}C	mult[a]	δattached H	HMBC correlations
1	34.5	CH	1.40 d	C-5, C-7, C-8
2	29.0	C[b]		
3	32.9	CH	2.08 dd	C-1, C-4, C-6
4	172.2	C[b]		
5	22.0	CH_3	1.14 s	C-1, C-2, C-3, C-6
6	20.3	CH_3	1.25 s	
7	120.7	CH	4.89 d	C-9, C-10
8	135.8	C[b]		
9	18.4	CH_3	1.71 s	C-7, C-8
10	25.5	CH_3	1.72 s	C-7, C-8
1′	72.9	CH	5.65 d	
2′	165.5	C[b]		
3′	141.9	C[b]		
4′	203.6	C[b]		
5′	42.0	CH_2	Hb, 2.85; Ha, 2.25 dd	C-2′, C-4′
6′	14.0	CH_3	2.04 s	C-2′, C-3′
7′	21.6	CH_2	3.12 d	C-3′, C-4′, C-8′, C-9′
8′	126.8	CH	5.36 dt	
9′	130.3	CH	6.04 dd	
10′	131.5	CH	6.72−6.81 m	
11′	118.2	CH_2	Ha, 5.17−5.23 dd; Hb, 5.32 br	

[a] Carbon multiplicities determined through DEPT (Doddrell et al., 1982). [b] Assignments based on HMBC (Bax and Summers, 1986).

Table 2. Summary of the Major Results of ^{1}H, ^{13}C, and HMBC Correlations of Pyrethrin II

position	δ^{13}C	mult[a]	δattached H	HMBC correlations
1	35.7	CH	1.75 d	
2	29.6	C[b]		
3	32.9	CH	2.21 dd	
4	172.3	C[b]		
5	22.3	CH_3	1.24 s	
6	20.4	CH_3	1.31 s	C-5
7	138.9	CH	6.47 d	C-10
8	143.0	C[b]		
9	30.5	CH_3	1.71 s	C-7, C-10
10	168.1	CH_3	1.72 s	
11	51.8	OCH_3	3.74 s	C-10
1′	73.4	CH	5.66 d	C-5′
2′	164.9	C[b]		
3′	142.2	C[b]		
4′	203.5	C[b]		
5′	41.9	CH_2	Hb, 2.92; Ha, 2.23 dd	C-2′, C-4′
6′	14.1	CH_3	2.04 s	C-2′, C-3′, C-4′
7′	21.7	CH_2	3.13 d	C-2′, C-3′, C-4′, C-8′, C-9′
8′	126.7	CH	5.35 dt	
9′	130.4	CH	6.05 dd	
10′	131.5	CH	6.73−6.82 m	
11′	118.4	CH_2	Ha, 5.18−5.23 dd; Hb, 5.27 br	C-9′

[a] Carbon multiplicities determined through DEPT (Doddrell et al., 1982). [b] Assignments based on HMBC (Bax and Summers, 1986).

patterns for the P**I** molecule were similar to those of P**II**. As noticeable in Figure 4, the most revealing cross-peaks of P**I** connected H-11′a with Me-9, Me-10, and H-3; H-11′b with Me-6; H-8′ with Me-5 and H-3; Hα-5′ with H-1; and H-7 with both Hα-5′ and Hβ-5′ protons. For P**II**, cross-peaks connecting H-11′a with MeCO, H-8′ with H-3, H-9′ with Me-5, Me-6′ with MeCO, H-9 with H-1, and H-7 with both Hα-5′ and Hβ-5′ protons provided valuable conformational information. Taken together, the NOE data suggest that P**I** and P**II** molecules, on an NMR time scale, adopt "love-seat" conformations in the relatively hydrophobic solvent

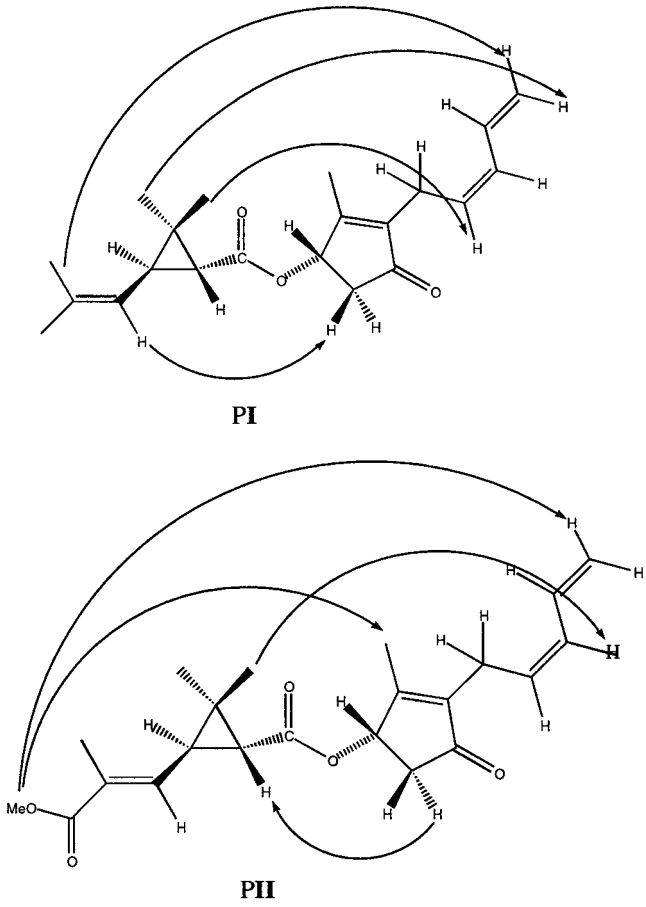

Figure 7. Diagnostic spatial correlations observed in the 2D NOESY spectra of P**I** and P**II**.

Table 3. Selected Distances (Å) of Pyrethrin I (PI) and Pyrethrin II (PII)

protons	P**I**	P**II**	protons	P**I**	P**II**
H-7, H-5	3.09	3.66	H-5′α, H-11′a	4.17	4.03
H-7, H-6	4.53	5.13	H-5′α, H-11′b	5.37	5.33
H-5, H-9	5.56	4.32	H-5′α, H-11	NA	11.18
H-5, H-10	5.41	NA[a]	H-5′α, H-8′	6.20	6.33
H-5, H-1′	6.69	6.70	H-5′β, H-1	5.17	5.63
H-5, H-6′	7.94	7.35	H-5′β, H-5	7.43	7.15
H-5, H-8′	10.77	8.95	H-5′β, H-6	5.84	4.65
H-5, H-9′	9.80	7.19	H-5′β, H-9	6.31	7.97
H-5, H-10′	8.77	5.93	H-5′β, H-10	9.19	NA
H-5, H-3	4.06	4.09	H-5′β, H-8′	6.61	6.67
H-5, H-11′a	7.85	3.78	H-5′β, H-11′a	6.61	5.63
H-5, H-11′b	8.37	4.75	H-5′β, H-11′b	6.87	6.64
H-6, H-9	6.19	4.45	H-6, H-7	4.53	5.13
H-6, H-10	7.22	NA	H-7, H-1	3.51	2.53
H-6, H-1′	4.44	5.26	H-7, H-9	4.01	3.97
H-6, H-6′	5.82	6.71	H-11′a, H-9	3.16	7.21
H-6, H-8′	9.37	8.24	H-11′a. H-10	5.82	NA
H-6, H-9′	9.12	7.12	H-11′a, H-6′	5.73	4.91
H-6, H-10′	8.18	4.60	H-11′b, H-9	3.11	8.60
H-6, H-3	3.10	3.14	H-11′b, H-10	5.47	NA
H-6, H-11′a	8.18	4.75	H-11′b, H-6	5.20	4.28
H-6, H-11′b	8.52	4.75	H-11, H-1	NA	7.59
H-6′, H-10′	4.61	4.30	H-11, H-6′	NA	12.63
H-6′, H-9	5.17	9.87	H-11, H-6	NA	8.85
H-6′, H-10	7.68	NA	H-11, H-5	NA	6.96
H-9′, H-5	9.80	7.19	H-11, H-11′a	NA	11.21
H-9′, H-6	9.12	7.12	H-11, H-1′	NA	11.52
H-5′α, H-9	4.82	6.93	H-1′, H-1	4.84	4.41
H-5′α, H-10	7.76	NA	H-3, H-8′	7.20	9.83
H-5′α, H-5	6.74	5.68	H-3, H-11′a	6.01	5.77
H-5′α, H-6	5.89	3.12	H-9′, H-6′	4.18	3.97

[a] NA, not applicable.

($CDCl_3$). For the first time, the methyl groups (Me-5 and Me-6) of cyclopropyl and vinyl *gem*-dimethyl groups

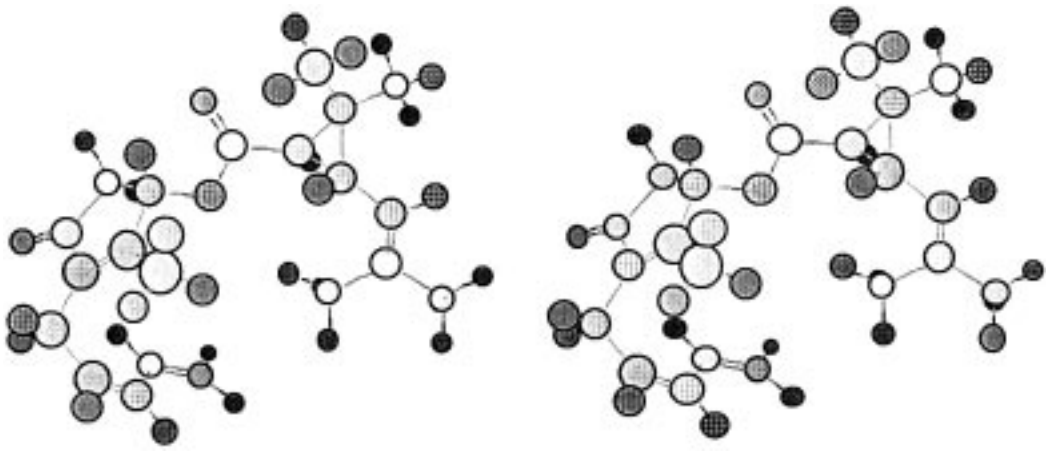

Figure 8. Stereoview of pyrethrin **I** based on molecular modeling calculations.

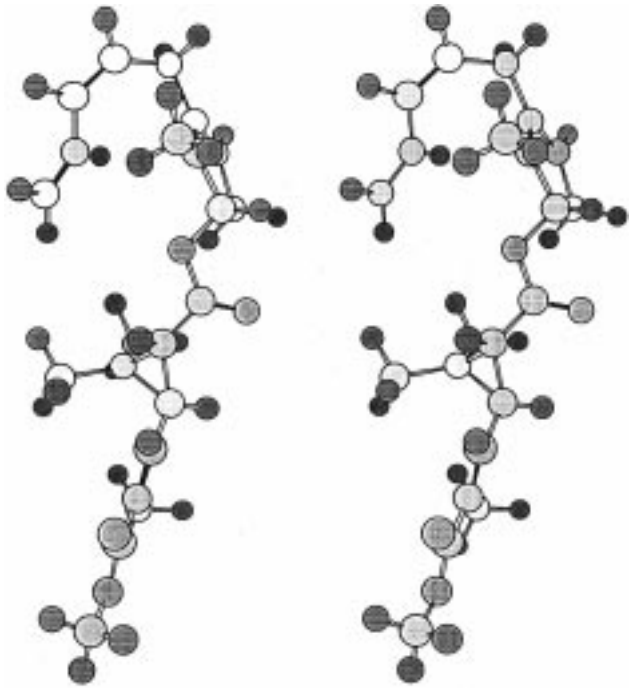

Figure 9. Stereoview of pyrethrin **II** based on molecular modeling calculations.

(Me-9 and Me-10) were unambiguously assigned using the 2D NOESY and HMBC experiments.

Conformational Analysis. Molecular mechanics is a powerful tool for probing the conformations of flexible molecules that are not detected by NMR. Recently, molecular modeling has been utilized for predicting biologically active conformations of natural products (Rugutt and Rugutt, 1997). Hitherto, most structure−activity studies have not yet yielded specific information about conformation(s) adopted by pyrethrins at the receptor sites of insects (Khambay et al., 1994; Kalyanasundaram, 1994). Elliot and Janes (1977) performed preliminary studies on the preferred conformations of pyrethroids using the Dreiding models. To further explain our NMR NOE data, several reasonable structures of P**I** and P**II** were modeled and subjected to energy minimization using the SYBYL 6.3 program. As can be seen in Figures 8 and 9, the most stable conformations of both esters have different geometries. The structural data (energy and selected distances are summarized in Table 3) were in agreement with the NOE data.

Table 4. Inhibition (%) of *M. tuberculosis* and *M. avium* by Crude Extracts and Different Fractions of Pyrethrum Flower

		% inhibition			
		M. tuberculosis		*M. avium*	
fraction	solvent ratio (hexane/EtOAc)[a]	100[b]	33[b]	100[b]	33[b]
crude[c]		94	56	94	53
1	100/0	0	0	0	6
2	90/10	72	7	98	83
3	80/20	89	51	99	88
4	70/30	93	46	99	96
5	60/40	74	47	96	94
6	50/50	84	67	88	64
7	40/60	85	55	93	58
8	30/70	76	28	88	55
9	20/80	9	0	31	11
10	10/90	0	5	0	0
11	0/100	0	0	0	11

[a] Solvent mixture (v/v). [b] In μg/mL. [c] Crude extract (bulk no. 9819-4).

Antimycobacterial Bioassays. It is well-known that the mycobacteria produce lipid-rich cell walls made up of a large amount of long hydrocarbon chains of C_{60}−C_{90} fatty acids (usually called mycolic acids) (Yuan and Barry III, 1996). The tight packing of mycolic acids (see structure **1**, in which $a = 17$, $b = 14$, $c = 13$, and $d = 21$) seriously limits the penetration of antibiotics into the cell walls.

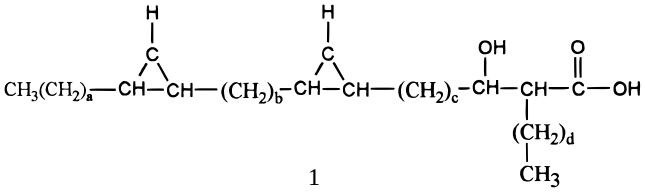

1

In the present study, an organic extract from the Kenyan pyrethrum flowers was subjected to VLC gradient elution using a solvent system of EtOAc−hexane (increasing amounts of EtOAc). Ten fractions were collected and bioassayed using the standard BACTEC technology with *M. tuberculosis* H37Rv and *M. avium* as test organisms. The percentage inhibition data indicated that most fractions exhibited activity at 33 and 100 μg/mL concentration levels (Table 4). The highest biological activities were in the fraction 3−8 range. There was little or no activity in the more polar (100% EtOAc) or nonpolar (100% hexane) fractions. The intermediate polar fractions (3 and 4) with a high degree

of inhibitions (46−99%) contained several isoprene long-chain alcohols (Combaut and Piovetti, 1983; Amico et al., 1987; Albrizio et al., 1992; Rugutt et al., 1998). The two most abundant and active intermediate fractions (5 and 6) were pooled and chromatographed (hexanes−EtOAc, 1:1 v/v) to afford P**I** and P**II** as the major constituents. Pure (>95% by NMR) P**I** and P**II** exhibited slight differences in their efficacies against *M. tuberculosis* H37Rv (MIC's of 64 and 32 μg/mL, respectively). Preliminary correlations of structural features and the MIC's suggest that the presence of an ester moiety in P**II** seems to enhance the in vitro antimycobacterial activity. The differences in the MIC's suggest that the similarity in structure is not a sufficient condition for antimycobacterial activity. Therefore, the structures of P**I** and P**II** do not necessarily represent the active conformers in solution. In comparison with the established antimycobacterial agents, the specific potency of P**I** and P**II**, while interesting, is sufficient to warrant detailed future studies. Further structural modifications and testing of natural pyrethrins is in progress in order to derive definitive clues on the active functional group(s) (Rugutt et al., 1999).

CONCLUSION

The conformational analysis of P**I** and P**II** by molecular modeling (MM) and NMR protocols not only provides new insights into their molecular modes of action but also forms a good starting point for the analysis of natural pyrethrins and other antimycobacterial agents.

ABBREVIATIONS USED

MM, molecular mechanics; P**I**, pyrethrin **I**; P**II**, pyrethrin **II**; C**I**, cinerin **I**; C**II**, cinerin **II**; J**I**, jasmolin **I**; J**II**, jasmolin **II**. NMR, nuclear magnetic resonance; 1D, one-dimensional; 2D, two-dimensional; COSY, correlation spectroscopy; NOESY, nuclear Overhauser effect spectroscopy; HMQC, heteronuclear quantum coherence; HMBC, heteronuclear multiple bond correlation; DEPT, distortionless enhancement polarization transfer; PΦ, polarization pulse angles; *J*, coupling constant; CH, methine; CH_2, methylene; CH_3, methyl; $CDCl_3$, deuterated chloroform; ^{1}H, proton; ^{13}C, carbon-13; VLC, vacuum−liquid chromatography; ppm, parts per million; ZQ, zero quantum; DQ, double quantum; GC/MS, gas chromatography/mass spectrometry; HPLC, high-performance liquid chromatography; MM, molecular modeling; eq, equation.

ACKNOWLEDGMENT

We thank Anita N. Biswas for performing bioassays and Dr. James M. Wangai, Messrs. Cleophas D. Ochieng, and Robinson M. Kuria of the Pyrethrum Board of Kenya for providing pyrethrum samples.

LITERATURE CITED

Albrizio, S.; Fattorusso, E.; Magno, S.; Mangoni, A. Linear diterpenes from the Caribbean sponge *Myrmekioderma styx*. *J. Nat. Prod.* **1992**, *55*, 1287−1293.

Amico, V.; Neri, P.; Piattelli, M.; Ruberto, G. Linear diterpenoids from *Cystoseira Balearica*. *Phytochemistry* **1987**, *26*, 2637−2639.

Bax, A.; Summers, M. F. ^{1}H and ^{13}C assignments from sensitivity-enhanced detection of heteronuclear multiple-bond connectivity by 2D multiple quantum NMR. *J. Am. Chem. Soc.* **1986**, *108*, 2093−2094.

Bax, A.; Davis, D. G. Practical aspects of two-dimensional transverse NOE spectroscopy. *J. Magn. Reson.* **1985**, *63*, 207−213.

Bramwell, A. F.; Crombie, L.; Hemesley, P.; Pattenden, G. Nuclear Magnetic Resonance Spectra of the natural pyrethrins and related compounds. *Tetrahedron* **1969**, *25*, 1727−1741.

Burkert, U.; Allinger, N. L. *Molecular Mechanics*; ACS Monograph 177; American Chemical Society: Washington, DC, 1982; pp 1−304.

Bullivant, M. J.; Pattenden, G. Photodecomposition of natural pyrethrins and related compounds. *Pestic. Sci.* **1976**, *7*, 231−235.

Burton, G. W.; Ingold, K. U. Vitamin E: Application of the principles of physical organic chemistry to the exploration of its structure and function. *Acc. Chem. Res.* **1986**, *19*, 194−201.

Casida, J. E. In *Pyrethrum—The Natural Insecticide*; Casida, J. E., Ed.; Academic Press: New York, 1973; pp 1−221.

Collins, L. A.; Franzblau, S. G. Microplate alamar blue assay versus BACTEC 460 system for high-throughput screening of compounds against *Mycobacterium avium*. *Antimicrob. Agents Chemother.* **1997**, *41*, 1004−1009.

Bystrov, V. F. Spin−spin coupling and the conformational states of peptide systems. *Prog. NMR Spec.* **1976**, *10*, 41−81.

Chen, Y.; Casida, J. Photodecomposition of pyrethrin I, allethrin, phthalthrin, and dimethrin. *J. Agric. Food Chem.* **1969**, *17*, 208−214.

Combaut, G.; Piovetti, L. Novel acyclic diterpene from the brown alga *Bifurcaria bifurcata*. *Phytochemistry* **1983**, *22*, 1787−1789.

Crombie, L.; Pattenden, G.; Simmonds, D. Carbon-13 Nuclear Magnetic Resonance spectra of the natural pyrethrins and related compounds. *J. Chem. Soc., Perkin 1* **1975**, 1500−1502.

Diehl, P.; Kellerhals, H.; Lustig, E. Computer assistance in the analysis of high-resolution NMR spectra. In *NMR: Basic Principles and Progress*; Diehl, P., Fluck, E., Kosfeld, R., Eds.; Springer-Verlag: New York, 1972; pp 1−96.

Doddrell, D. M.; Pegg, D. T.; Bendall, M. R. Distortionless enhancement of NMR signals by polarization transfer. *J. Magn. Reson.* **1982**, *48*, 323−327.

Doskotch, R. W.; El-Feraly, F. S.; Hufford, C. Sesquiterpene lactones from pyrethrum flowers. *Can. J. Chem.* **1971**, *49*, 2103−2109.

Elliot, M. The Pyrethroids: Early discovery, recent advances and the future. *Pestic. Sci.* **1989**, *27*, 337−351.

Elliot, M.; Janes, N. F. Preferred conformations of pyrethroids. In *Synthetic Pyrethroids*; Gould, R. F., Ed.; ACS Symposium Series; American Chemical Society: Washington, DC, 1977; Chapter 2, pp 29−36.

Elliot, M.; Farnham, A.; Janes, N.; Needham, P.; Fulman, D. Insecticidally active conformations of pyrethroids. *Active Conformations of Pyrethoids.* **1974**, *6*, 80−91.

Fesik, S. W. In *Computer-Aided Drug Design, Methods and Applications*; Perun, T. J., Propst, C. L., Eds.; Marcel Dekker: New York; 1989; pp 56−91.

Grange, J. M.; Davey, R. W. Detection of antituberculosis activity in plant extracts. *J. Appl. Bacteriol.* **1990**, *68*, 587−591.

Heifets, L. B. *Drug Susceptibility in the Chemotherapy of Mycobacterial Infections*; CRC Press: Boca Raton, FL, 1991; Chapter 3, pp 89−121.

Houston, S.; Fanning, A. Current and potential treatment of tuberculosis. *Drugs* **1994**, *48*, 689−708.

Inderlied, C. B.; Kemper, C. A.; Bermudez, L. E. M. The *Mycobacterium avium* complex. *Clin. Microbiol. Rev.* **1993**, *6*, 266−310.

Iseman, M. D. Evolution of drug-resistant tuberculosis: a tale of two species. *Proc. Natl. Acad. Sci. U.S.A.* **1994**, *91*, 576−578.

Jackson, L. M.; Sternhell, S. *Applications of Nuclear Magnetic Resonance Spectroscopy in Organic Synthesis*, 2nd ed.; Pergamon Press: Oxford, 1962; pp 292−298.

Johnston, J.; Horsham, M.; Class, T.; Casida, J. Metabolites of the prototype insecticide (2*E*,4*E*)-*N*-Isobutyl-6-phenylhexa-2,4-dienamide. 2. Formation in mouse and rat liver microsomal systems, rat hepatocytes, and houseflies. *J. Agric. Food Chem*. **1989**, *37*, 781−786.

Kalyanasundaram, M. Chemistry of synthetic pyrethroid insecticides—Some recent advances. *J. Sci. Ind. Res*. **1994**, *53*, 933−945.

Karimi-Nejad, Y.; Schmidt, J. M.; Ruterjans, H.; Schalbe, H.; Griesinger, C. Conformation of valine side chains in Ribonuclease T_1 determined by NMR studies of homonuclear and heteronuclear ^3J coupling constants. *Biochemistry* **1994**, *33*, 5481−5492.

Karplus, M. Vicinal proton coupling in NMR. *J. Am. Chem. Soc*. **1963**, *85*, 2870.

Karplus, M. Contact electron-spin coupling of nuclear magnetic moments. *J. Chem. Phys*. **1959**, *30*, 11−15.

Kessler, H.; Gehrke, M.; Griesinger, C. Two-dimensional NMR Spectroscopy: Background and Overview of the Experiments. *Angew. Chem., Int. Ed. Engl*. **1988**, *27*, 490−536.

Kessler, H.; Bermel, M. Methods in stereochemical analysis. In *Applications of NMR spectroscopy to Problems in Stereochemistry and Conformational Analysis*; Takenchi, Y., Marchand, A. P., Eds.; VCH Press: Dedfield Beach, 1986; pp 179−205.

Khambay, B. P. S.; Farnham, A. W.; Beddie, D. G. Relationships between pyrethroid structure and level of resistance in Houseflies (*Musca domestica* L.). In *Advances in the Chemistry of Insect Control III*; Briggs, G. G., Ed.; AgrEvo UK Ltd: Saffron Walden, Essex, UK. Royal Society of Chemistry, 1994; p 117.

Krishnamurthy, V. V.; Cassida, J. E. COLOC-S: a Modified COLOC sequence for selective Long-Range X−H Correlation 2D NMR spectroscopy. *Magn. Reson. Chem*. **1987**, *25*, 837−842.

Mahato, S. B.; Banerjee, S. Steroid transformations by microorganisms-II. Review article number 8. *Phytochemistry* **1985**, *24*, 1403−1421.

McEldowney, A. M.; Menary, R. C. Analysis of pyrethrins in pyrethrum extracts by High-Performance Liquid Chromatography. *J. Chromatogr*. **1988**, *447*, 239−243.

Miskus, R.; Andrews, T. Stabilization of thin films of pyrethrins and allethrin. *J. Agric. Food Chem*. **1972**, *20*, 313−315.

Otieno, D.; Jondiko, I.; McDowell, P.; Kezdy, F. Quantitative Analysis of the Pyrethrins by HPLC. *J. Chromatogr. Sci*. **1982**, *20*, 566−570.

Pattenden, G.; Crombie, L.; Hemesley, P. The mass spectra of the pyrethrins and related compounds. *Org. Mass Spectrom*. **1973**, *7*, 719−735.

Pelletier, S. W.; Chokshi, H. P.; Desai, H. K. Separation of diterpenoid mixtures using vacuum liquid chromatography. *J. Nat. Prod*. **1986**, *49*, 892−900.

Rance, M.; Sørensen, O. W.; Bodenhausen, G.; Wagner, R. R.; Ernst, R. R.; Wüthrich, K. Improved spectral resolution in COSY ^{1}H NMR spectra of proteins via double quantum filtering. *Biochem. Biophys. Res. Commun*. **1983**, *117*, 479−485.

Rastogi, N.; Frehel, C.; Ryter, A.; Ohayon, H.; Lesourd, M.; Davide, H. L. Multiple drug resistant in *Mycobacterium avium*: is the wall architecture responsible for the exclusion of antimicrobial agents? *Antimicrob. Agents Chemother*. **1981**, *20*, 666−667.

Rugutt, J. K.; Franzblau, S. G.; Warner, I. M. Efficacy of crude organic extracts and pure compounds against *Mycobacterium tuberculosis* and *M. avium*. In preparation.

Rugutt, J. K.; Shamsi, S. A.; Aucoin, A. M.; Warner, I. M.; Franzblau, S. G. Activity of chiral surfactants against *Mycobacterium tuberculosis*. Presented at Pittcon, New Orleans, Louisiana, March 1−5, 1998; Abstract 1046.

Rugutt, J. K.; Berner, D. K. Activity of extracts from nonhost legumes on the germination of *Striga hermonthica* seeds. *Phytomedicine* **1998**, *5*, 293−299.

Rugutt, J. K.; Rugutt, K. J. Stimulation of *Striga hermonthica* seed germination by 11β,13- Dihydroparthenolide. *J. Agric. Food Chem*. **1997**, *45*, 4845−4849.

Rugutt, J. K.; Fischer, N. H.; Nauman, M. A.; Schmidt, T. J.; Bener, D. K. Carbon-13 assignments and revision of the stereostructures of the cadinanes 2-Hydroxy-8α-angeloxycalamenene and 2-Hydroxy-8α-hydroxycalamenene. *Spectrosc. Lett*. **1996**, *29*, 799−818.

Secoy, D. M.; Smith, A. E. Use of plants in control of agricultural and domestic pests. *Econ. Bot*. **1983**, *37*, 28−57.

Seebach, D.; Ciceri, P. E.; Overhand, M.; Jaun, B.; Rigo, D.; Oberer, L.; Hommel, U.; Amstutz, R.; Widmer, H. 170. Probing the helical secondary structure of short-chain β-peptides. *Helv. Chim. Acta*. **1996**, *79*, 2043−2066.

Sundaram, K. M.; Curry, J. Effects of some UV light absorbers on the photostability of azadirachtin, a Neem-based biopesticide. *Chemosphere* **1996**, *32*, 649−659.

"*SYBYL" 6.3*, TRIPOS force field; TRIPOS Association, Inc.: 1699 S. Hanley Rd, St. Louis, MO 63144, 1991.

Touchstone, J. C. Thin-layer chromatographic procedures for lipid separation. *J. Chromatogr. B* **1995**, *671*, 169−195.

Ueda, K.; Gaughan, L. C.; Casida, J. E. Photodecomposition of resmethrin and related pyrethroids. *J. Agric. Food Chem*. **1974**, *22*, 212−220.

Ueda, K.; Matsui, M. Studies on chrysanthemic acid-XXI: Photochemical isomerization of chrysanthemic acid and its derivatives. *Tetrahedron* **1971**, *27*, 2771−2774.

Van Den Thillart, G.; Van Waarde, A. Nuclear magnetic resonance spectroscopy of living systems: Applications in comparative physiology. *Physiol. Rev*. **1996**, *76*, 799−837.

Wayne, L. G. Dormancy of *Mycobacterium tuberculosis* and latency of disease. *Eur. J. Clin. Microbiol. Infect. Dis*. **1994**, *13*, 908−914.

Yuan, Y.; Barry, C. E., III. A common mechanism for the biosynthesis of methoxy and cyclopropyl mycolic acids in *Mycobacterium tuberculosis*. *Proc. Natl. Acad. Sci. U.S.A*. **1996**, *93*, 12828−12833.

Received for review June 17, 1998. Revised manuscript received May 14, 1999. Accepted May 17, 1999. I.M.W. acknowledges financial support from the National Institutes of Health (Grant GM 39844) and the Philip W. West endowment.

JF980660B